

Magnetic monopole plasma phase in (2+1)d compact quantum electrodynamics with fermionic matter

Wesley Armour^{a,b}, Simon Hands^c, John B. Kogut^{d,e}, Biagio Lucini^c,
Costas Strouthos^{f1} and Pavlos Vranas^g

^a*Diamond Light Source, Harwell Campus, Didcot,
Oxfordshire OX11 0DE, United Kingdom*

^b*Institute for the Future of Computing, Oxford Martin School,
Oxford e-Research Centre, 7 Keble Road,
Oxford OX1 3QG, United Kingdom*

^c*Department of Physics, College of Science,
Swansea University, Singleton Park, Swansea SA2 8PP, United Kingdom*

^d*Department of Energy, Division of High Energy Physics,
Washington, DC 20585, USA*

^e*Department of Physics, University of Maryland, 82 Regents Drive,
College Park, Maryland 20742, USA*

^f*Computation-based Science and Technology Research Center,
The Cyprus Institute, 1645 Nicosia, Cyprus*

^g*Lawrence Livermore National Laboratory, Livermore, CA 94550, USA*

Abstract

We present the first evidence from lattice simulations that the magnetic monopoles in three dimensional compact quantum electrodynamics (cQED₃) with $N_f = 2$ and $N_f = 4$ four-component fermion flavors are in a plasma phase. The evidence is based mainly on the divergence of the monopole susceptibility (polarizability) with the lattice size at weak gauge couplings. A weak four-Fermi term added to the cQED₃ action enabled simulations with massless fermions. The exact chiral symmetry of the interaction terms forbids symmetry breaking lattice discretization counter-terms to appear in the theory's effective action. It is also shown that the scenario of a monopole plasma does not depend on the strength of the four-Fermi coupling. Other observables such as the densities of “isolated” dipoles and monopoles and the so-called specific heat show that a crossover from a dense monopole plasma to a dilute monopole gas occurs at strong couplings. The implications of our results on the stability of $U(1)$ spin liquids in two spatial dimensions are also discussed.

¹Corresponding author. E-mail address: strouthos@ucy.ac.cy

1 Introduction

Gauge field theories play an important role in both high energy and condensed matter physics. The mechanism of quark confinement in gauge theories with dynamical fermions such as QCD remains one of the most elusive subjects in particle physics. As a result, model field theories play a significant role in studying this phenomenon. Three dimensional parity-invariant compact quantum electrodynamics is such an interesting and challenging field theory with rich dynamics that resemble four-dimensional QCD. It is an asymptotically free theory, because the gauge coupling e^2 has mass dimension one and thus provides the theory with a natural scale that plays the role of Λ_{QCD} in four dimensions. Polyakov in his pioneering work on quenched cQED₃ [1] showed analytically that static electric charges are confined via a linear potential for arbitrarily small values of the gauge coupling. More specifically, he showed via duality of electric and magnetic monopole-like instanton charges that the model is equivalent to a three-dimensional Coulomb monopole gas described by a sine-Gordon effective action; this in turn leads to a nonzero photon mass and area law for the Wilson loop [2].

The situation is less clear when cQED₃ is coupled to N_f massless four-component fermionic flavors, because the interaction between monopoles and antimonopoles is changed by the vacuum polarization. A simple way of seeing why massless fermions might be expected to have a dramatic effect is to observe that as a result of the Dirac quantization condition the combination eg (g is the charge of the magnetic monopole) is a renormalization group (RG) invariant [3]. Given that the renormalized electron charge $e_R < e$ due to screening by e^-e^+ virtual pairs then the renormalized monopole charge $g_R > g$. Hence, virtual e^-e^+ pairs antiscreen the monopole-antimonopole ($m\bar{m}$) interaction. If the monopoles are in plasma phase at least for small N_f values, then based on the dual superconductor model [4, 5] the electric charges are linearly confined. In gauge field theories the particles of the vacuum that are analogous to the electrons of the superconductor are the magnetic monopoles. The monopoles set up magnetic currents which confine the electric field between the charges into a narrow flux tube, in a similar way to the electric currents around magnetic flux tubes in an ordinary superconductor. Since this narrow flux tube has a constant energy/length, it gives rise to a linearly confining potential.

The issue of the (non-)existence of a monopole plasma phase in cQED₃ coupled to N_f massless fermionic flavors has been addressed analytically by various authors. Different approaches often based on perturbative renormalization group (RG) analysis of an approximate dual anomalous sine-Gordon (ASG) action led to different results depending on the type of approximations in the calculations. Using an electrostatic argument and an RG calculation the authors of [6] claimed that the interactions among magnetic dipoles screen the logarithmic $m\bar{m}$ potential for arbitrarily large but finite N_f back into the Coulomb form at large distances. This result was confirmed by a self-consistent variational analysis of the dual ASG theory [7]. The results of [6, 7] were criticised by the authors of [8] who showed in a systematic RG analysis that for large N_f the monopole operators are irrelevant in the infrared limit and the physics of the system is controlled by a conformally invariant fixed point (in the context of cuprate

superconductors discussed later in this section it is known as the algebraic spin liquid). Arguments based on analysis of topological symmetries [9] produced results consistent with [8]. In addition, the authors of [10] claimed that for $N_f \geq 2$ the average size of the $m\bar{m}$ dipoles collapses to zero leading to non-compact QED₃, provided the fermions are massless. If the fermions have a small mass then the monopoles are in a dipolar phase. In a more recent RG calculation the authors of [11] claimed that for $N_f > N_f^{\text{crit}} = 36$ the fermions are deconfined, for $20 < N_f \leq 36$ they can be either confined or deconfined, depending on the monopole density and for $N_f \leq 20$ the fermions are confined.

Lattice simulations provide a reliable non-perturbative tool for studying the role of magnetic monopoles in cQED₃. So far, there have not been any simulations that address directly the (non-)existence of a monopole plasma phase in cQED₃. The inclusion of massless fermions in the compact $U(1)$ gauge action makes simulations difficult due to the non-local interactions generated when integrating over fermionic variables. Therefore, the authors of [12] addressed the issue of electric charge confinement in cQED₃ via lattice simulations of an effective $U(1)$ lattice gauge theory with a variety of nonlocal interactions in the time-like direction that mimic the effects of gapless/gapful matter fields. The main result of [12] is that for certain power-law decaying interactions (mimicking coupling to massless matter fields) a second order phase transition separates a confined from a deconfined phase. The existence of a deconfined phase in the effective theory indicates that when cQED₃ is coupled to a large number of massless matter fields the theory may be in the deconfined phase. It has been also shown with Monte Carlo simulations [13] that charged particles with $\ln(r)$ interactions exhibit a phase transition at a critical temperature T_c between a dilute dipole gas and a monopole plasma. This result also provides indirect evidence that monopoles in cQED₃ may be in a dipolar phase above a certain N_f^{crit} .

In this paper we present the first attempt to resolve the controversy in the analytical literature via lattice simulations of cQED₃ with $N_f = 2$ and $N_f = 4$. Massless fermion simulations were enabled with the inclusion of a weak (unable to break chiral symmetry on its own) four-Fermi term in the theory's action. The results that are largely based on the diverging monopole susceptibility (polarizability) with the lattice extent L at weak couplings imply that the monopoles are in a plasma phase. The details of the lattice model including the role of the four-Fermi interaction are discussed in Sec. 2. Recent simulations of non-compact QED₃ (ncQED₃) with an extra weak four-fermi term [14] showed that the magnetic charges (which unlike in cQED₃ they are not classical solutions of the theory) form tightly bound $m\bar{m}$ dipoles, because in this case the Dirac strings carry a non-vanishing contribution to the pure gauge (non-compact) part of the action [15]. The different monopole dynamics in lattice cQED₃ and ncQED₃ for $N_f \leq 4$ at weak gauge couplings imply that the two models have different continuum limits. The authors of [16, 17] performed simulations of both cQED₃ and ncQED₃ with $N_f = 2$ at strong gauge couplings and concluded that the two formulations may be equivalent. This suggestion was largely based on comparisons of chirally extrapolated data for the chiral condensate versus monopole density which appeared to collapse on the same curve for the two QED₃ formulations. A similar claim was presented for weak couplings [17] based on simulations with a lattice size $L = 32$. These results, however, are questionable given

that $N_f = 2$ ncQED₃ simulations with $L = 50$ [18] and later on with $L = 80$ [19] did not provide any evidence for the existence of a nonzero chiral condensate. The principal obstruction to a definite answer in ncQED₃ is the large separation of scales in the theory, i.e. the fermion dynamical mass is at least an order of magnitude smaller than the natural cutoff scale e^2 . In addition, large finite volume effects resulting from the presence of a massless photon in the spectrum prevent a reliable extrapolation to the thermodynamic limit. So far, the evidence from lattice simulations of ncQED₃ is that $N_f^{\text{crit}} < 1.5$ [19, 20]. It should be noted though, that recent lattice simulations of ncQED₃ with an additional weak four-Fermi term [14] hinted at evidence that chiral symmetry may be broken up to $N_f = 4$. Analytical results based on self-consistent solutions of Schwinger-Dyson equations (SDE) [21, 22] claimed that to detect chiral symmetry breaking for $N_f \geq 1.5$ lattice volumes much bigger than the ones currently used in simulations are required. The most recent SDE-based analytical calculations showed that $N_f^{\text{crit}} \approx 4$ [21, 23]. In addition, a gauge invariant calculation based on the divergence of the chiral susceptibility resulted in $N_f^{\text{crit}} = 2.2$ [24] and an RG approach on QED₃ with extra irrelevant four-Fermi interactions resulted in $N_f^{\text{crit}} = 6$ [25]. An alternative approach based on simulations of the $(2 + 1)d$ Thirring model at infinite coupling which may belong to the same universality class as ncQED₃ resulted in $N_f^{\text{crit}} = 6.6(1)$ [26].

Although cQED₃ is a model field theory used for studying elementary particle physics phenomena, and is also an interesting basic field theory on its own right, it acquires more concrete phenomenological significance in condensed matter physics, because $(2 + 1)d$ field theories with a compact $U(1)$ gauge field coupled to gapless relativistic fermions arise as low energy effective field theories in two dimensional strongly correlated electron systems, such as the cuprate superconductors [27, 28, 29, 30]. Strong interactions lead to correlated electron motion resulting in unconventional states of matter with “fractionalized” quantum numbers where the quasiparticle approach of Landau’s Fermi liquid theory is not valid. It is well-known from experiments that, for cuprates, the Mott insulating state at zero doping is the Néel antiferromagnetic state but the nature of the connection between the undoped Mott state and the doped d -wave superconductor is still under theoretical debate. In a specific incarnation of Anderson’s [31] resonating valence bond idea, it was proposed [28, 29] that the so-called $U(1)$ spin liquids are the phases of matter that play a significant role in understanding underdoped cuprates. These featureless quantum paramagnetic states with no broken symmetries or long-range order, also known as critical or algebraic spin liquids (ASL), behave as if the system is at a critical point without the fine-tuning of any parameter. The physical picture can be visualized in terms of valence bonds between pairs of spin singlets separated by arbitrarily large distances and the unpaired charge-neutral gapless spin $1/2$ spinons interact strongly with the valence bond background. The flux of the emergent $U(1)$ gauge field arises from extra topological conservation laws not present in the microscopic theory [32]. In a low energy description of $U(1)$ spin liquids, the spinons with a linear dispersion are coupled minimally to an emergent compact $U(1)$ gauge field, resulting in cQED₃. Of particular importance to the physics of cuprates is the so-called staggered flux (or d -wave resonating valence bond) phase which is formally described by cQED₃ (the anisotropy of the interactions is neglected) with $N_f = 2$ four-component fermions.

Another ASL with an important role in strongly correlated electron systems is the so-called π -flux state, which is described by $N_f = 4$ cQED₃. Ghaemi and Senthil [33] showed that the staggered flux spin liquid state may be connected to the Nèel antiferromagnetic state via a second order quantum phase transition. For extensive reviews on high T_c superconductivity resulting from doping a Mott insulator we refer the reader to [34] and references therein. These spin liquid phases are stable provided the magnetic monopoles are not in a plasma phase and hence are unable to induce linear spinon confinement. In addition to the works mentioned in a previous paragraph regarding the role of magnetic monopoles in cQED₃ [6, 7, 8, 9, 10, 11], Alicea [35] found a monopole operator which represents a symmetry allowed perturbation, and speculated that this may destabilize the staggered flux phase leading to charge confinement. The numerical evidence presented in this paper in favor of the existence of a monopole plasma phase for $N_f \leq 4$ implies that both the staggered-flux and the π -flux spin liquids are unstable to spinon linear confinement. This in turn leads to Nèel antiferromagnetic order where the chiral condensate $\langle \bar{\psi}\psi \rangle$ corresponds to the staggered magnetization. It should also be noted that in a more phenomenological approach an anisotropic version of ncQED₃ has been proposed for the phase fluctuations in the pseudogap phase (also known as algebraic Fermi liquid phase) of cuprate superconductors [36].

This paper is organized as follows: In Sec. 2 we present the lattice model, the various monopole observables, and the simulations parameters. In Sec. 3 we present and discuss the simulation results and in Sec. 4 we present our conclusions and also point to possible future expansions of this project.

2 The Model

In this first numerical exploration of the role of magnetic monopoles in cQED₃ with an additional four-Fermi term we have chosen the simplest Z_2 chirally symmetric four-Fermi interaction which for practical purposes is preferable over terms with a continuous chiral symmetry, because the latter are not as efficiently simulated due to the presence of massless modes in the strongly cut-off theory. For computational purposes it is useful to introduce the auxiliary field $\sigma \equiv g_s^2 \bar{\chi}_i \chi_i$ (summation over the index i is implied), where $\chi_i, \bar{\chi}_i$ are $\frac{N_f}{2}$ -component staggered fermion fields and g_s^2 is the four-Fermi interaction coupling. The lattice action in terms of real-valued link potentials $\theta_{\mu\nu}$ is given by the following equations:

$$S = \sum_{i=1}^{N_f/2} \left(\sum_{x,x'} \bar{\chi}_i(x) Q(x, x') \chi_i(x') \right) + \frac{N_f \beta_s}{4} \sum_{\tilde{x}} \sigma_{\tilde{x}}^2 + \beta \sum_{x, \mu < \nu} (1 - \cos \Theta_{\mu\nu x}), \quad (1)$$

where

$$\begin{aligned} \Theta_{\mu\nu x} &\equiv \theta_\mu(x) + \theta_\nu(x + \mu) - \theta_\mu(x + \nu) - \theta_\nu(x), \\ Q(x, x') &\equiv \frac{1}{2} \sum_{\mu} \eta_\mu(x) [e^{i\theta_\mu(x)} \delta_{x', x+\mu} - e^{-i\theta_\mu(x)} \delta_{x', x-\mu}] + \delta_{xx'} \frac{1}{8} \sum_{\langle \tilde{x}, x \rangle} \sigma(\tilde{x}) + m \delta_{xx'}. \end{aligned} \quad (2) \quad (3)$$

The indices x, x' consist of three integers (x_1, x_2, x_3) labelling the lattice sites, where the third direction is considered timelike. The symbol $\langle \tilde{x}, x \rangle$ denotes the set of the eight dual lattice sites \tilde{x} surrounding the direct lattice site x , where the σ field lives [37]. The $\eta_\mu(x)$ are the Kawamoto-Smit staggered fermion phases $(-1)^{x_1+\dots+x_{\mu-1}}$, designed to ensure relativistic covariance of the Dirac equation in the continuum limit. The inverse gauge and four-Fermi couplings are given by $\beta \equiv \frac{1}{e^2 a}$ and $\beta_s \equiv \frac{a}{g_s^2}$, respectively, and a is the physical lattice spacing. The boundary conditions for the fermion fields are antiperiodic in the timelike direction and periodic in the spatial directions. In the weakly coupled ($\beta \rightarrow \infty$) long-wavelength limit eq. (1) describes N_f four-component Dirac fermions [38].

Performing simulations with massless fermions even with the reduced Z_2 chiral symmetry has substantial advantages, both theoretical and practical. The theory has the exact symmetry of the interaction terms, which forbid chiral symmetry breaking counterterms from appearing in its effective action. In addition, because of the large nonzero vacuum expectation value of the σ field at strong gauge couplings² or its fluctuations at weak couplings, the Dirac operator is nonsingular even with $m = 0$ and its inversion is very fast. Another advantage of simulations with $m = 0$, is that we do not have to rely on often uncontrolled $m \rightarrow 0$ extrapolations to calculate various observables in chiral limit. For these reasons both the non-compact and compact lattice versions of the theory have been successfully simulated in $(3+1)d$ [39, 40] and showed that QED₄ is a logarithmically trivial theory and the systematics of the logarithms follow those of the Nambu–Jona-Lasinio model rather than those of the scalar $\lambda\phi^4$ as often assumed. Unlike $(3+1)d$ where the four-Fermi term is a marginally irrelevant operator, in $(2+1)d$ it is a relevant operator. It is well-known that the $(2+1)d$ Gross-Neveu model (GNM₃) although non-renormalizable in the weak coupling perturbation theory, is renormalizable in the $1/N_f$ expansion [41]. At sufficiently strong couplings chiral symmetry is spontaneously broken, leading to a dynamically generated fermion mass $\Sigma \approx \langle \sigma \rangle \gg m$. The interacting continuum limit of the theory may be taken at the critical coupling g_{sc}^2 (at which the gap $\Sigma/\Lambda_{UV} \rightarrow 0$), which defines an ultraviolet-stable renormalization group fixed point.

In QED₃, as the gauge coupling is varied (with the four-Fermi coupling kept fixed at some weak value $g_s^2 < g_{sc}^2$), depending on the value of N_f the model is expected to undergo either a chiral phase transition or a sharp crossover from a strong coupling phase (where $\langle \bar{\chi}\chi \rangle \neq 0$) to a weak coupling phase where $\langle \bar{\chi}\chi \rangle$ is either zero or very small and possibly undetectable in lattice simulations. Hereafter, we will use the term “chiral transition” to denote either a chiral phase transition or a sharp crossover from strong to weak gauge couplings. Near the transition the weak four-Fermi term is expected to play a dominant role as compared to the ultraviolet-finite gauge interaction. Simulations of ncQED₃ [14] showed that the order parameter scales with critical exponents close to those of GNM₃ and the scaling region is suppressed by a factor $\sim g_s$. The GNM₃ scaling is expected to be valid for both compact and non-compact lattice formulations. It should also be noted that in the large- N_f and $\beta \rightarrow \infty$ limits the four-Fermi term is

²At strong couplings, pure QED₃ simulations are dramatically slowed down by the strong gauge field fluctuations.

an irrelevant operator in the RG sense [25].

The simulations were performed with the standard Hybrid Molecular Dynamics (HMD) R algorithm. We used conservatively small values for the HMD trajectory time-step dt and ensured that any $\mathcal{O}(dt^2)$ systematic errors are smaller than the statistical errors for different observables. For lattice sizes smaller than or equal to 24^3 we used $dt = 0.005$ and an HMD trajectory length $\tau = 1$ and for 32^3 we used $dt = 0.0025$ with a trajectory length $\tau = 2$.

The magnetic monopoles in the lattice model are identified following the standard DeGrand and Toussaint approach [42]. The plaquette angles $\Theta_{\mu\nu}$ are written as

$$\Theta_{\mu\nu} = \bar{\Theta}_{\mu\nu} + 2\pi s_{\mu\nu}(x), \quad (4)$$

where $\bar{\Theta}_{\mu\nu}$ lie in the range $(-\pi, \pi]$ and $s_{\mu\nu}(x)$ is an integer that determines the flux due to a Dirac string passing through a plaquette. The gauge invariant integer number of monopole charges on the dual lattice sites \tilde{x} are then given by

$$M(\tilde{x}) = \epsilon_{\mu\nu\lambda} \Delta_\mu^+ s_{\nu\lambda}(\tilde{x}), \quad (5)$$

where Δ_μ^+ is the forward lattice derivative and $M \in \{0, \pm 1, \pm 2\}$. Since on a three-torus the total magnetic charge $\sum_{\tilde{x}} M(\tilde{x}) = 0$ we define the density of monopole charges as

$$\rho_M = \frac{1}{V} \sum_{\tilde{x}} |M(\tilde{x})|. \quad (6)$$

The mere counting of monopoles does not provide any useful information on whether their presence has any impact on the model's confining properties. As already discussed in Sec. 1 a monopole plasma is required for linear confinement of electric charges.

The observable that provides information on whether the monopoles are in a plasma or a dipolar phase is the monopole susceptibility χ_m [43]:

$$\chi_m = - \sum_r \langle r^2 M(0) M(r) \rangle. \quad (7)$$

The susceptibility is the polarizability of the monopole configurations; this can be readily seen by adding a uniform magnetic field term $-B \sum_r r M(r)$ to the dual monopole action [43] and evaluating $\chi_m = \partial^2 \ln \mathcal{Z} / \partial^2 B|_{B=0}$, where \mathcal{Z} is the monopole partition function. If the magnetic charges are in a plasma phase, then χ_m diverges with the lattice size L , implying that external magnetic fields are shielded. A finite χ_m means that monopoles and antimonopoles form a polarized gas of $m\bar{m}$ dipoles, which is what was observed in ncQED₃ simulations [14]. The situation may be very different in cQED₃, where the monopoles are classical solutions of the theory and they may exist in a plasma phase at least for small N_f values. Results from numerical simulations of cQED₃ with $N_f = 2$ and $N_f = 4$ presented in Sec. 3 favor the existence of a monopole plasma phase. Also, as shown in [44], in the infinite volume limit further manipulations lead to a form of χ_m expressed as a Fourier transform of a two-point correlation function at zero wavevector:

$$\chi_m \propto \sum_x \langle \bar{\Theta}_{\mu\nu}(x) \bar{\Theta}_{\mu\nu}(0) \rangle \propto \sum_x \langle s_{\mu\nu}(x) s_{\mu\nu}(0) \rangle. \quad (8)$$

The observable χ_m has been rarely measured in simulations with dynamical fermions, because it is very noisy due to near cancellations of monopole-monopole and monopole-antimonopole contributions. With the inclusion of the four-fermi term in the QED₃ action the algorithm became very efficient and χ_m has been measured with an acceptable signal-to-noise ratio at weak gauge couplings. We generated $\approx 10^5 - 2 \times 10^5$ configurations for the largest $L = 32$ lattice and $\approx 3 \times 10^5 - 7 \times 10^5$ configurations for the smaller lattices ($L = 8, \dots, 24$).

We also measured χ_1 given by

$$\chi_1 = -\langle M(0)M(1) \rangle, \quad (9)$$

which includes the contributions in χ_m from adjacent lattice cubes only. In addition, we measured χ_2 given by

$$\chi_2 = -\sum_{r \leq \sqrt{3}} \langle r^2 M(0)M(r) \rangle, \quad (10)$$

which includes the terms of χ_m where two neighboring magnetic charges share either a cube face, an edge or a corner. $\chi_1 \approx \chi_2 \approx \chi_m$ indicates that the main contribution to χ_m comes from tightly bound $m\bar{m}$ pairs. Therefore, a comparison of χ_m with χ_1 and χ_2 provides information on whether the monopole configurations are dominated by tightly bound dipoles or not. This will become clearer in Sec. 3 where we compare the behavior of these observables (as a function of L) for both cQED₃ and ncQED₃.

3 Results

In this section we present results from simulations of the lattice model in eq. (1) with $N_f = 2$ and $N_f = 4$ fermion flavors. Before presenting data for the monopole observables we present results for the chiral condensate $\langle \bar{\chi}\chi \rangle$ versus β near the $N_f = 4$ strong coupling chiral transition. In the infinite gauge coupling limit ($\beta \rightarrow 0$), it is known rigorously that chiral symmetry is broken [45] for values of N_f below a certain critical value. Simulations of QED₃ with staggered fermions and $\beta = 0$ showed that the theory undergoes a second-order phase transition at $N_f \approx 8$ [46]. With the extra weak four-Fermi term the infinite gauge coupling transition is shifted towards larger N_f values, depending on the value of β_s . Therefore, in cQED₃ as β increases and N_f is larger than a putative N_f^{crit} (for $N_f > N_f^{\text{crit}}$ the monopoles are in the dipolar phase) there must exist a chiral phase transition at some critical value of the gauge coupling β_c . For $N_f < N_f^{\text{crit}}$, since the chiral order parameter is small at weak gauge couplings, the relic of the transition may persist as a sharp crossover between weak and strong couplings with a tail of exponentially suppressed $\bar{\chi}\chi$ extending to weak couplings. The bulk of the simulations presented in this paper were performed with a fixed $\beta_s = 2.0$, which is larger than the critical coupling $\beta_s^{\text{crit}} = 0.835(1)$ for the three-dimensional $N_f = 4$ GNM₃ (and hence larger than β_s^{crit} for $N_f = 2$ GNM₃). Therefore, the four-Fermi term with $\beta_s = 2.0$ cannot break chiral symmetry on its own. However, as already mentioned in Sec. 2, in three dimensions the weak four-Fermi term is expected to play a dominant

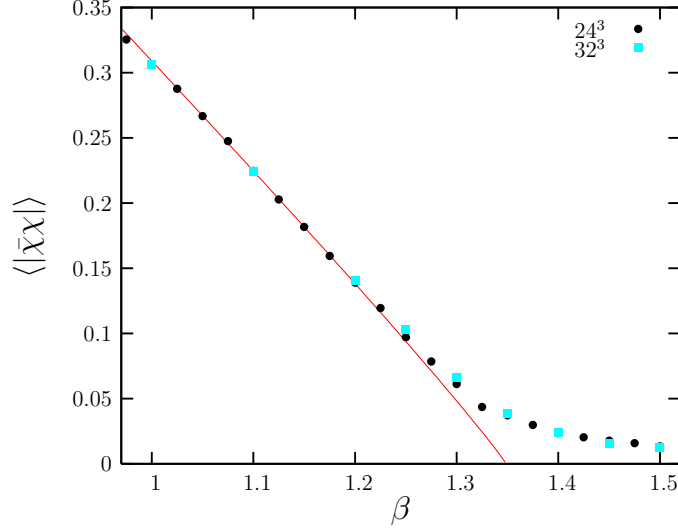


Figure 1: (Color online) $\langle |\bar{\chi}\chi| \rangle$ vs β extracted from simulations with $N_f = 4$ on 24^3 and 32^3 lattices. The solid curve represents the fitting function (eq. (11)) for $\beta \in [1.025, 1.200]$.

Table 1: Values of $\langle |\bar{\chi}\chi| \rangle$ for $N_f = 4$ from simulations on 24^3 and 32^2 lattices near the crossover.

β	$\langle \bar{\chi}\chi \rangle_{24}$	$\langle \bar{\chi}\chi \rangle_{32}$
1.30	0.0612(9)	0.0658(17)
1.35	0.0372(11)	0.0383(15)
1.40	0.0236(3)	0.0238(10)
1.45	0.0178(5)	0.0154(9)
1.50	0.0134(5)	0.0125(9)
1.60	0.0112(2)	0.0080(2)

role near the chiral transition as compared to the ultraviolet-finite gauge interaction. It was shown in simulations of ncQED₃ [14] that the critical exponents extracted for the $N_f = 4$ transition are close to the GNM₃ ones, and small deviations hinted at evidence for nonzero fermion mass generated by the gauge field dynamics. On a finite volume lattice near the transition the values of $\bar{\chi}\chi$ may change sign due to tunnelling events between the Z_2 vacua resulting $\langle \bar{\chi}\chi \rangle = 0$. In order to take into account these tunnelling events and following similar analyses of the Ising model we measured the effective order parameter $\langle |\bar{\chi}\chi| \rangle$ instead of $\langle \bar{\chi}\chi \rangle$. We fitted the data extracted from simulations with $L = 24$ for $\langle |\bar{\chi}\chi| \rangle$ versus β to the standard scaling relation for a second-order phase transition order parameter

$$\langle |\bar{\chi}\chi| \rangle = A(\beta_c - \beta)^{\beta_m}. \quad (11)$$

For the fitting range $\beta \in [1.025, 1.200]$ we obtained $\beta_c = 1.35(1)$ and $\beta_m = 0.94(3)$ with an acceptable fit quality given by $\chi^2/\text{DOF} = 1.8$. The extracted value of β_m is in very good agreement with the $\beta_m = 0.93(3)$ of $N_f = 4$ GNM₃ [47]. The GNM₃ scaling confirms our earlier assertion that the exact chiral symmetry of the lattice action forbids

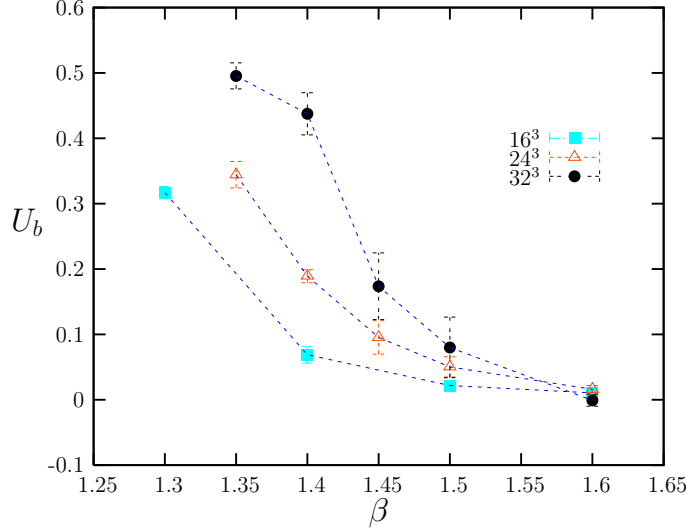


Figure 2: (Color online) Binder's cumulant vs β for $L = 16, 24, 32$ near the $N_f = 4$ chiral crossover.

symmetry breaking lattice discretization counterterms from appearing in the model's free energy. The 24^3 data (together with some 32^3 data) and the fitted curve are shown in Fig. 1. By expanding the fitting window towards larger values of β , the value of β_m increased and the fit quality deteriorated. The fit quality deteriorated dramatically when data points above $\beta = 1.35$ were included. If, however, $\beta = 1.35$ were a critical coupling then one would expect the effective order parameter to obey the finite size scaling relation $\langle |\bar{\chi}\chi| \rangle \sim L^{\beta_m/\nu} \approx L^{-0.93}$ ($\beta_m/\nu = 0.927(15)$ in $N_f = 4$ GNM₃ [47]). However, as shown in Table 1, instead of observing a decrease of $\langle |\bar{\chi}\chi| \rangle$ with L at the putative critical coupling $\beta = 1.35$ we observe that for $\beta = 1.35, 1.40$ the values of the effective order parameter on 24^3 and 32^3 are equal within statistical errors. The values of $\langle |\bar{\chi}\chi| \rangle$ for $\beta = 1.45, 1.50$ from the two lattices also agree within 1-2 standard deviations. Finally at $\beta = 1.60$ which corresponds to the weakest gauge coupling in Table 1 large finite volume effects (the physical volume shrinks with β) result in $\langle |\bar{\chi}\chi| \rangle_{32} < \langle |\bar{\chi}\chi| \rangle_{24}$. These observations together with the failure of eq. (11) to provide acceptable fits when weak couplings were included in the fitting window constitute serious evidence that instead of a chiral phase transition we have a crossover from strong to weak couplings. It should be noted that in ncQED₃ although we observed small deviations of the exponents from the GNM₃ ones, above the transition there was a decrease of $\langle |\bar{\chi}\chi| \rangle$ with L , possibly because any tiny non-zero chiral condensate is “swallowed” by finite volume effects. This difference between the two lattice QED₃ formulations could be attributed to the different magnetic monopole dynamics, i.e. in cQED₃ the monopoles may be in a plasma phase, which in turn leads to an enhanced chiral condensate. Before concentrating on the role of monopoles in cQED₃, we will study the behavior of the Binder cumulant $U_b(\beta, L)$ [48] defined by

$$U_b \equiv 1 - \frac{\langle (\bar{\chi}\chi)^4 \rangle}{3\langle (\bar{\chi}\chi)^2 \rangle^2}, \quad (12)$$

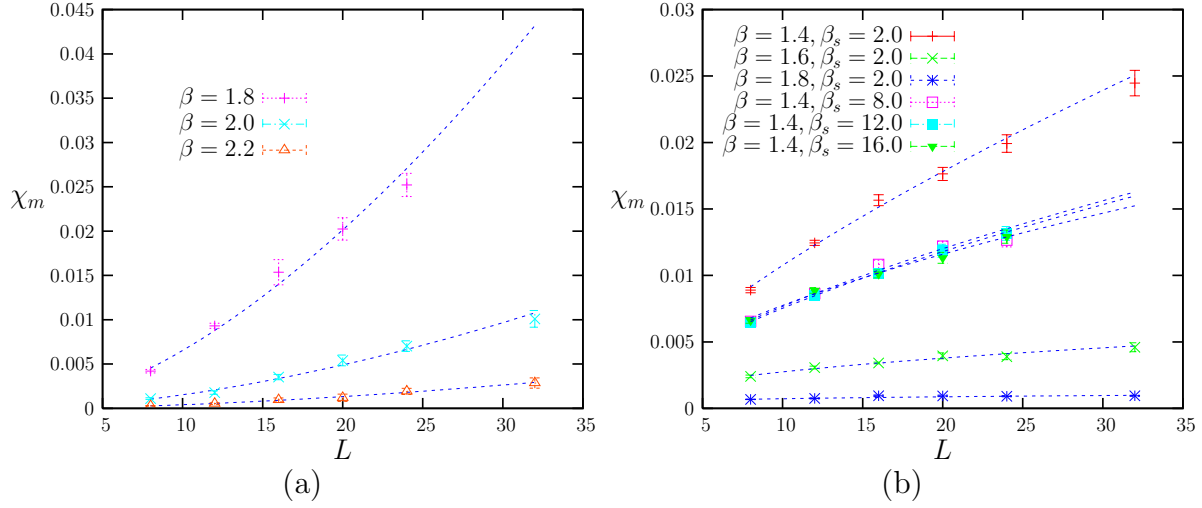


Figure 3: (Color online) χ_m vs. L for (a) $N_f = 2$, and (b) $N_f = 4$. The fitting functions (eq. (13)) are represented by solid lines.

and measured on different lattice sizes near the chiral crossover. Near a second order phase transition and with sufficiently large lattices (where subleading corrections from finite L are negligible) $U_b = f_b((\beta_c - \beta)L^{1/\nu})$. Therefore, at a critical coupling the lines connecting data of the same L are expected to cross at a universal value $U_b = U_b^*$. In a symmetric phase as $L \rightarrow \infty$ $U_b \rightarrow 0$. For $N_f = 4$ GNM₃ $U_b^* = 0.232(8)$ [26]. In Fig. 2 we present $U_b(\beta, L)$ data for $N_f = 4$ cQED₃ with $L = 16, 24, 32$. Although U_b is a lot noisier than the effective order parameter it is clear that the lines joining data with the same L do not cross for $\beta < 1.45$. This observation provides additional evidence in favor of the crossover scenario instead of a phase transition for $\beta < 1.5$. The crossings of the constant L U_b lines occur at $\beta \approx 1.6$ where the values of U_b are less than 0.02. As stated earlier even if for $\beta \geq 1.6$ chiral symmetry is broken, the physical lattice volume is smaller and therefore it is plausible that finite size effects make the phase look as if it is symmetric.

Next, we turn our attention to the role of magnetic monopoles. As discussed in Sec. 2, the most relevant observable for deciding whether the monopoles are in a plasma or a dipolar phase is the monopole susceptibility χ_m . Its short distance contributions χ_1 and χ_2 elucidate further the situation. It is instructive to compare data for these observables from both the compact and non-compact lattice formulations of QED₃. Recent ncQED₃ simulations [14] showed that the magnetic charges form tightly bound $m\bar{m}$ dipoles. In Figures 3 (a) and (b) we present the χ_m results at weak gauge couplings for $N_f = 2$ and $N_f = 4$, respectively. The data are fitted to a power-law relation

$$\chi_m = cL^\alpha \quad (13)$$

and the extracted values of the exponent α are shown in Fig. 4. The clear increase of

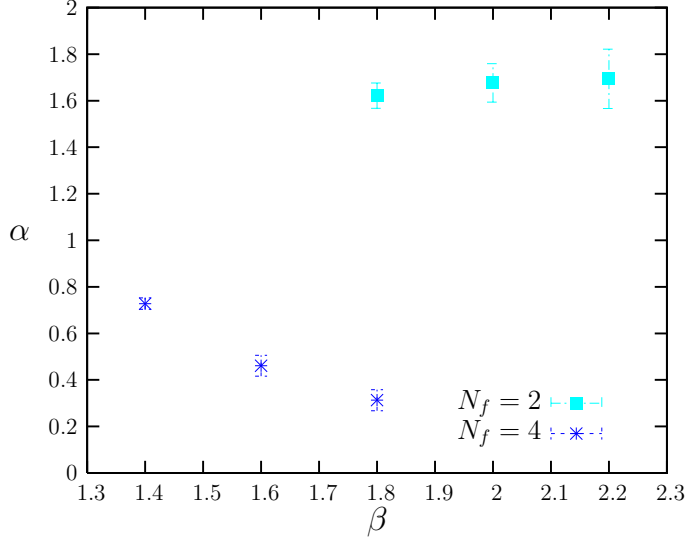


Figure 4: (Color online) Exponent α vs. β extracted from fits with eq. (13) for $N_f = 2$ and $N_f = 4$.

χ_m with L in Fig. 3 and the non-zero values of the exponent α in Fig. 4 imply that the magnetic charges are in a plasma phase. As expected, the values of α for $N_f = 2$ are larger than those for $N_f = 4$. This can be understood in terms of the renormalization group invariant Dirac quantization condition $eg = e_R g_R = n/2$ (n is an integer and the subscript R denotes renormalized charges): As N_f increases the e^+e^- interaction decreases due to enhanced screening from virtual fermion-antifermion pairs, which in turn implies that the $m\bar{m}$ interaction is antiscreened. In addition the $N_f = 4$ values of α appear to decrease with β . It is possible that for large N_f values, the extracted values of α may be affected by finite size effects. This can be understood as follows: The interaction among magnetic dipoles leads to a screening of the $m\bar{m}$ interaction [6, 7], resulting in a small density of unbound magnetic charges. This mechanism implies that the existence of a monopole plasma may be a very long distance effect. Therefore, simulations on larger lattices may be required in order to extract more accurate values of α . The existence of the monopole plasma depends solely on the gauge field dynamics and it is not expected to depend on the four-Fermi coupling provided the latter is weak enough. This is supported by the $\beta_s > 2.0$ data in Fig. 3 (b). The data for $\beta_s = 8.0, 12.0, 16.0$ from simulations with $L = 8, \dots, 24$ almost collapse on a single curve and the values of α for the three different β_s are consistent with $\alpha = 0.61(7)$ which is close to the $\beta_s = 2.0$ value $\alpha = 0.73(3)$. The slightly smaller value of α in the $\beta_s \rightarrow \infty$ limit could be attributed to the fact that the additional four-Fermi term enhances the e^-e^+ interaction, implying an enhanced antiscreening effect on the $m\bar{m}$ interaction.

At this point it is worth comparing data for χ_m from both cQED₃ and ncQED₃. In Fig. 5 we present χ_m versus L for ncQED₃ above the chiral transition/crossover for $N_f = 2, 4$, $\beta_s = 2.0$ and $\beta = 0.4, 0.5$. The horizontal lines give excellent fit qualities, implying that the values of χ_m do not depend on L , because the magnetic charges are in the dipolar phase.

In Figures 6 (a) and (b) we plot χ_m together with its short distance contributions χ_1

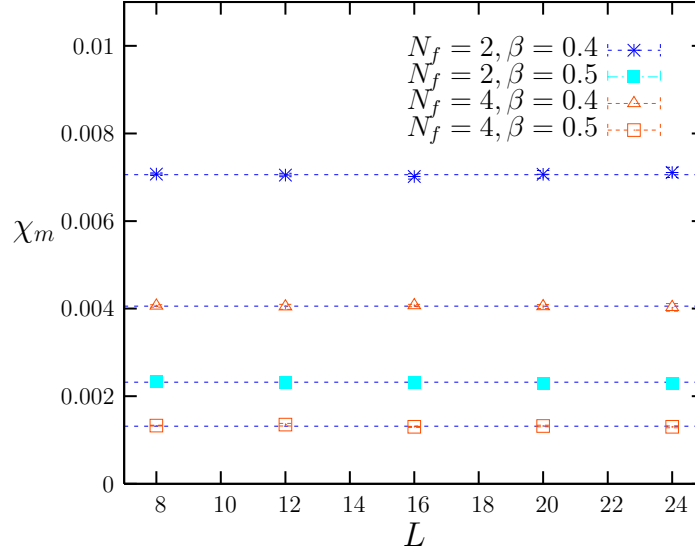


Figure 5: (Color online) χ_m vs. L for ncQED₃ with $N_f = 2, 4$ and $\beta = 0.4, 0.5$. The horizontal lines represent fits to the data.

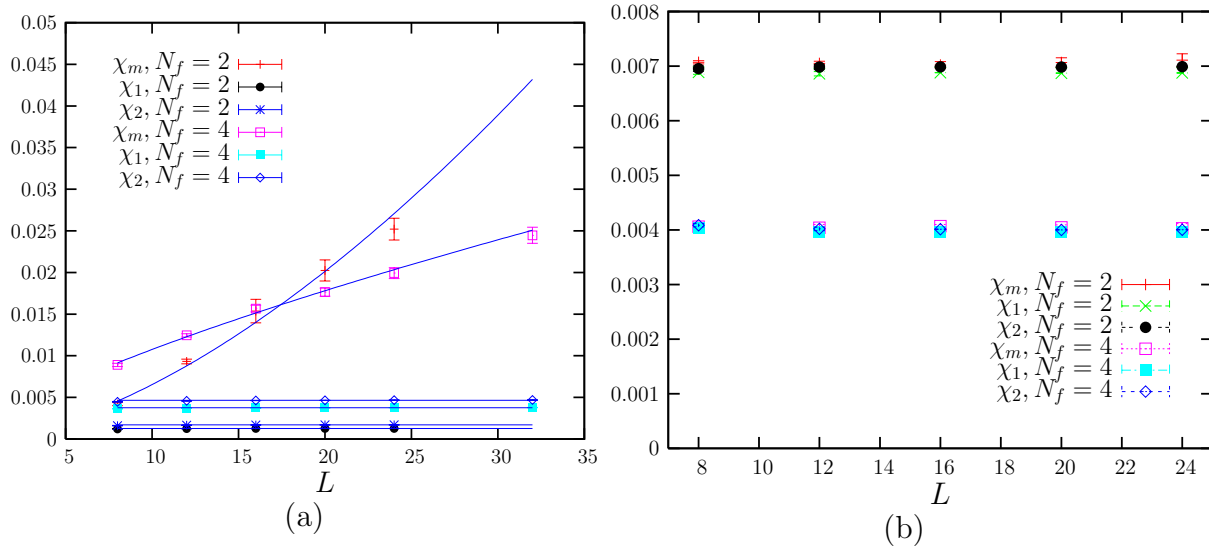


Figure 6: (Color online) χ_m , χ_1 , and χ_2 vs. L for (a) cQED₃ with $N_f = 2, \beta = 1.8$ and $N_f = 4, \beta = 1.4$ and (b) ncQED₃ with $N_f = 2, 4$ and $\beta = 0.4$.

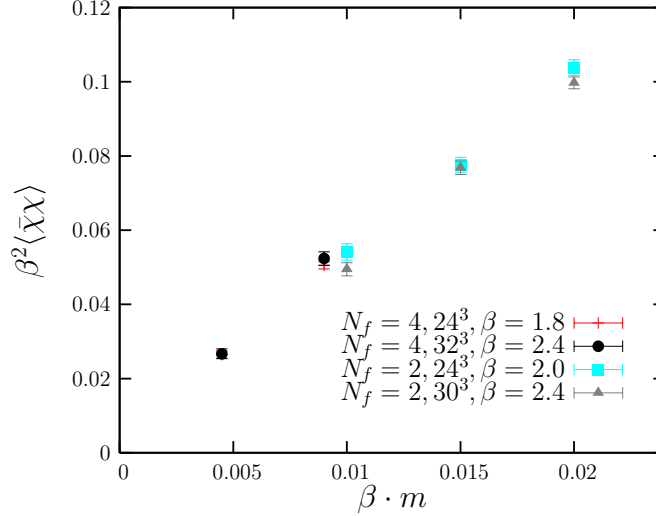


Figure 7: (Color online) $\beta^2 \langle \bar{\chi} \chi \rangle$ vs βm for $N_f = 2$, $N_f = 4$ at different values of the coupling β . The physical volume $(L/\beta)^3$ is constant for each N_f value.

and χ_2 versus L for cQED₃ and ncQED₃, respectively. For cQED₃, the χ_1 and χ_2 data fall on different horizontal lines below χ_m , because the divergence of χ_m which is a signature for a monopole plasma comes from long distance contributions. In contrast to this, the ncQED₃ data for χ_1 , χ_2 and χ_m coincide within statistical errors. This confirms that in ncQED₃ the contribution to the polarizability comes from tightly bound $\bar{m}m$ dipoles which in the continuum ($\beta \rightarrow \infty$) limit may disappear by collapsing into zero size.

Next, we check whether the gauge couplings $\beta = 2.0$ and $\beta = 1.8$ are in the asymptotic scaling regimes for $N_f = 2$ and $N_f = 4$, respectively. Since for an asymptotically-free field theory the ultraviolet behavior is governed by the gaussian fixed point at the origin, then the continuum limit of the model lies in the limit $\beta \rightarrow \infty$, and all physical quantities should be expressible in terms of the scale set by the dimensionful coupling e^2 . To compare simulation results taken at different couplings (lattice spacings), therefore, it is natural to work in terms of dimensionless variables such as βm , L/β , and $\beta^2 \langle \bar{\chi} \chi \rangle$. As the continuum limit is approached, data taken at different β should collapse onto a single curve when plotted in dimensionless units. To check whether lattice data are characteristic of the continuum limit we plot the dimensionless chiral condensate $\beta^2 \langle \bar{\chi} \chi \rangle$ versus the dimensionless fermion bare mass βm for $N_f = 2$ (with $\beta = 2.0$, $L = 24$ and $\beta = 2.4$, $L = 30$) and $N_f = 4$ (with $\beta = 1.8$, $L = 24$ and $\beta = 2.4$, $L = 32$) in Fig. 7. For both $N_f = 2$ and $N_f = 4$, the values of $\beta^2 \langle \bar{\chi} \chi \rangle$ for the two values of β agree within 1-2 standard deviations, implying that lattice discretization effects are small.

In order to complete the picture presented in the previous paragraphs we also measured various densities: (i) the density ρ_d of “isolated” tightly bound dipoles, which are $m\bar{m}$ pairs on adjacent cubes, and each charge in the dipole does not share any other cube face with with a second opposite charge; (ii) the density ρ_1 of positive magnetic charges that do not share a cube face with an antimonopole; and (iii) the density ρ_2 of “isolated” positive magnetic charges, that not share a cube face, an edge or a corner

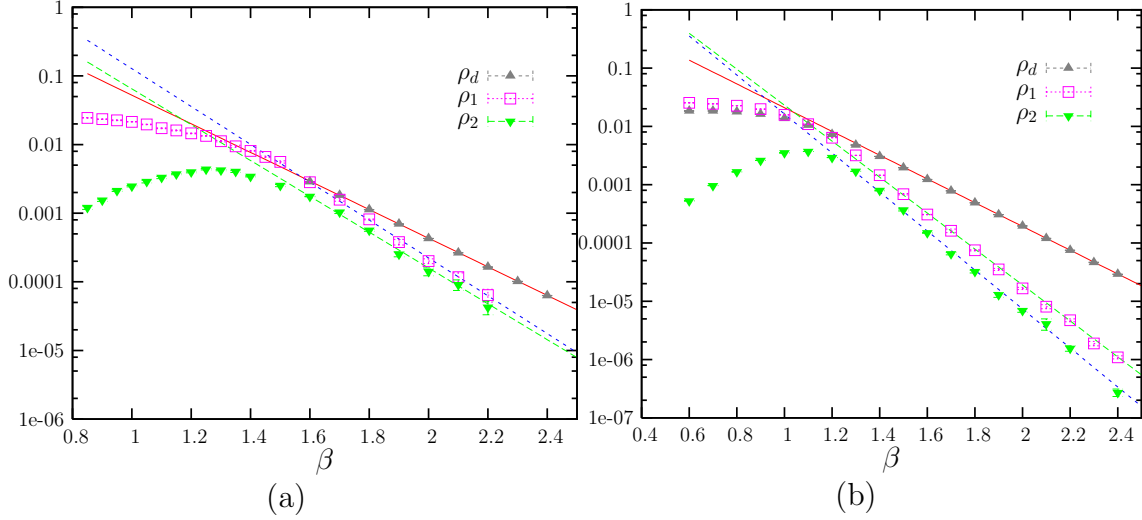


Figure 8: (Color online) ρ_d , ρ_1 , and ρ_2 vs. β for (a) $N_f = 2$, and (b) $N_f = 4$.

with an opposite charge. We fitted the data for ρ_d , ρ_1 and ρ_2 versus β to an exponential function $f(\beta) = a_1 \exp(-a_2 \beta)$. The data and the fitted curves for $N_f = 2$ and $N_f = 4$ are shown in Figures 8 (a) and (b), respectively. The results are from simulations on 32^3 lattices and a comparison with data on 24^3 lattices showed that finite volume effects are negligible. It is clear from the peak values of ρ_2 that a crossover from a dense monopole plasma phase at strong couplings to a dilute monopole gas at weak couplings occurs. The values of the crossover couplings are $\beta \approx 1.25$ and $\beta \approx 1.10$ for $N_f = 2$ and $N_f = 4$, respectively. The values of a_2 are presented in Table 2. The fact that the exponential function accurately fits the data implies that there is no phase transition that would result in an abrupt decrease of the densities. As expected, the values of the parameter a_2 for the “isolated” monopoles are a bit larger than the respective one in quenched cQED₃ where $a_2 \approx 5$ [42], whereas for the “isolated” dipoles the values of a_2 are smaller than the quenched value $a_2 = 6.6$ [42]. The crossover from a dense monopole plasma to a dilute monopole gas is also supported by the behavior of the so-called specific heat C_v defined in a way analogous to the specific heat in spin models (with the temperature T

Table 2: Values of parameter a_2 extracted from fits of $f(\beta) = a_1 \exp(-a_2 \beta)$ on ρ_d , ρ_1 and ρ_2 vs. β data.

N_f	2	4
$a_2(\rho_d)$	4.800(4)	4.660(3)
$a_2(\rho_1)$	6.4(1)	7.13(5)
$a_2(\rho_2)$	6.0(1)	7.8(1)

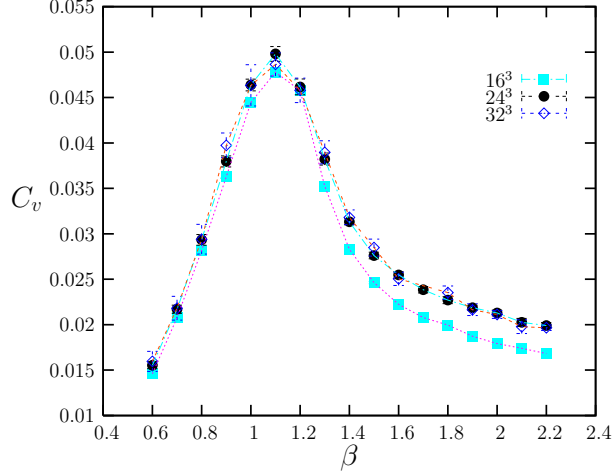


Figure 9: (Color online) Specific heat C_v vs. β for $N_f = 4$ and $L = 16, 24, 32$.

interchanged with the gauge coupling g^2) as follows:

$$C_v = -\beta^2 \frac{\partial \langle P \rangle}{\partial \beta} = \beta^2 \frac{\partial^2 \ln \mathcal{Z}}{\partial \beta^2} = \beta^2 [\langle P^2 \rangle - \langle P \rangle^2], \quad (14)$$

where \mathcal{Z} is the lattice partition function and $P \equiv \frac{1}{V} \sum_{x, \mu < \nu} (1 - \cos \Theta_{\mu\nu x})$ is the pure gauge part of the action per unit volume. In Fig. 9 we plot C_v versus β for $N_f = 4$ and $L = 16, 24, 32$. It is clear that C_v develops a lattice size-independent peak at $\beta = 1.1$. The L -independent peak of C_v implies that a smooth crossover takes place in the gauge field dynamics at $\beta = 1.1$, which coincides with the crossover from a dense monopole plasma to a dilute monopole gas.

4 Conclusions and Outlook

cQED₃ is an interesting field theory due to its similarities with QCD and its close relation with QCD-like theories [49]. In this paper we presented the first analysis of monopole dynamics in cQED₃ with $N_f \leq 4$ based on results from lattice simulations. Fast simulations with massless fermions were enabled by adding a weak four-Fermi interaction to the cQED₃ action, because the vacuum expectation value of the σ meson field which appears explicitly in the semi-bosonized action acts like a fermion mass and makes the Dirac matrix inversion fast. In addition, in the presence of the four-Fermi term the action has an exact Z_2 chiral symmetry, which forbids symmetry breaking lattice discretization counterterms in the free energy.

The monopole susceptibility (polarizability) diverges with the lattice extent, implying that the monopoles are in a plasma phase, which in turn leads to linear confinement of electric charges. Simulations at a single value of β for $N_f = 4$ showed that the monopole plasma scenario does not depend on the four-Fermi coupling β_s when β_s is sufficiently large. The cQED₃ results for the monopole susceptibility were contrasted with ncQED₃ data where χ_m is independent of L and its major contribution comes from charges on

adjacent lattice cubes, implying that the single lattice spacing size dipoles at finite β may collapse to zero size in the continuum limit. In addition, the behavior of the effective chiral order parameter $\langle |\bar{\chi}\chi| \rangle$ for $N_f = 4$ implies that a crossover instead of a transition takes place at strong couplings, which could be an outcome of a $V(r) \sim r$ electric potential. Also, the behavior of the density of “isolated” monopoles favors a scenario of a crossover from a dense plasma of monopoles to a dilute monopole gas at weak couplings. This scenario is supported by the L -independent peak of the so-called specific heat. Our results imply that for $N_f \leq 4$ the continuum limits of cQED₃ and ncQED₃ are different, with linear charge confinement for the former and logarithmic confinement for the later provided that $N_f = 4$ is below the ncQED₃ N_f^{crit} .

Our conclusions are supported by the results of [50], where it was shown that an isolated magnetic charge has an infinite free energy, both for the dynamical and the quenched system. Following similar lines, we plan to test the response of the system to the insertion of a static dipole. A vanishing free energy gap would confirm our results that monopoles are in a neutral plasma phase.

The existence of a monopole plasma phase in cQED₃ has implications in strongly correlated electron systems. More specifically $U(1)$ spin liquids (staggered-flux spin liquid corresponds to $N_f = 2$ and π -flux spin liquid to $N_f = 4$) in two spatial dimensions which are believed to describe the underdoped Mott insulator regime in cuprate superconductors may be unstable to spinon confinement. It should be noted, however, that the anisotropic interactions of these condensed matter systems have been neglected in our model. Recent analytical [51] and numerical [52] results of ncQED₃ with Fermi and gap anisotropies showed that the velocity anisotropy is relevant in the RG sense and its increase leads to a decrease of N_f^{crit} .

We are currently expanding the cQED₃ simulations to larger N_f values. The plan is to search for a putative conformally invariant fixed point at N_f^{crit} where a phase transition from a linearly confining phase to conformal deconfined phase may take place. In the condensed matter language this critical point would correspond to a deconfined quantum critical point [53], where a phase transition is expected to occur between a phase with Néel antiferromagnetic order (at small N_f) and a paramagnetic critical spin liquid phase (at large N_f). In addition, as emphasized in [34] $(2+1)d$ two-color QCD may provide a more appropriate description of algebraic spin liquids than cQED₃ which only includes Gaussian fluctuations about the mean field and suffers from various limitations in the underdoped regime. The study of the phase diagram of $(2+1)d$ two-color QCD is another non-perturbative problem that requires lattice simulations for reaching definitive answers.

Acknowledgements

The authors wish to thank the Diamond Light Source for kindly allowing them to use extensive computing resources and the Oxford University Supercomputing Centre for computing time on the ORAC supercomputer. The work of B.L. is supported by the Royal Society through the University Research Fellowship scheme. B.L. also acknowl-

edges partial financial support by STFC under contract ST/G000506/1.

References

- [1] A. M. Polyakov, Nucl. Phys. **B120**, 429 (1977).
- [2] T. Banks, R. Myerson, and J. B. Kogut, Nucl. Phys. **B129**, 493 (1977).
- [3] G. Calucci and R. Jengo, Nucl. Phys. **B223**, 501 (1983).
- [4] G. 't Hooft, in ‘High Energy Physics’, Proceedings of the EPS International Conference, Palermo 1975, ed. A. Zichichi (Editrice Compository, Bologna, 1976); G. 't Hooft, Nucl. Phys. **B190**, 455 (1981).
- [5] S. Mandelstam, Phys. Rep. **23**, 245 (1976).
- [6] I. F. Herbut and B. H. Seradjeh, Phys. Rev. Lett. **91**, 171601 (2003).
- [7] M. J. Case, B. H. Seradjeh and I. F. Herbut, Nucl. Phys. **B676**, 572 (2004).
- [8] M. Hermele, T. Senthil, M. P. A. Fisher, P. A. Lee, N. Nagaosa and X.-G. Wen, Phys. Rev. B **70**, 214437 (2004).
- [9] M. Ünsal, arXiv:0804.4664v1 [cond-mat.str-el].
- [10] C. D. Fosco and L. E. Oxman, Ann. Phys. **321**, 1843 (2006).
- [11] F. S. Nogueira and H. Kleinert, Phys. Rev. B **77**, 045107 (2008).
- [12] G. Arakawa, I. Ichinose, T. Matsui and K. Sakakibara, Phys. Rev. Lett. **94**, 211601 (2005); G. Arakawa, I. Ichinose, T. Matsui, K. Sakakibara and S. Takashima, Nucl. Phys. **B732**, 401 (2006).
- [13] S. Kragset, A. Sudbø, and F. S. Nogueira, Phys. Rev. Lett. **92**, 186403 (2004); K. Børke, S. Kragset, and A. Sudbø, Phys. Rev. B **71** 085112 (2005).
- [14] W. Armour, J. B. Kogut and C. Strouthos, Phys. Rev. D **82**, 014503 (2010).
- [15] S. Hands and R. Wensley, Phys. Rev. Lett. **63**, 2169 (1989).
- [16] H. R. Fiebig and R.M. Woloshyn, Phys. Rev. D **42**, 3520 (1990).
- [17] R. Fiore, P. Giudice, D. Giuliano, D. Marmottini, A. Papa and P. Sodano, Phys. Rev. D **72**, 094508 (2005).
- [18] S. J. Hands, J. B. Kogut and C. G. Strouthos, Nucl. Phys. **B645**, 321 (2002).
- [19] C. Strouthos and J. B. Kogut, PoS **LAT2007**, 278 (2007); C. Strouthos and J. B. Kogut, J. Phys. Conf. Ser. **150**, 052247 (2009).

- [20] S. J. Hands, J. B. Kogut, L. Scorzato and C. G. Strouthos, Phys. Rev. B **70**, 104501 (2004).
- [21] T. Goecke, C. S. Fischer and R. Williams, Phys. Rev. B **79**, 064513 (2009).
- [22] V. P. Gusynin and M. Reenders, Phys. Rev. D **68**, 025017 (2003).
- [23] P. Maris, Phys. Rev. D **54**, 4049 (1996); C. S. Fischer, R. Alkofer, T. Dahm, and P. Maris, Phys. Rev. D **70**, 073007 (2004).
- [24] M. Franz, T. Pereg-Barnea, D. E. Sheehy, Z. Tešanović, Phys. Rev. B **68**, 0245508 (2003).
- [25] K. Kaveh and I. F. Herbut, Phys. Rev. B **71**, 184519 (2005).
- [26] S. Christofi, S. Hands and C. Strouthos, Phys. Rev. D **75**, 101701 (2007).
- [27] D. H. Kim and P. A. Lee, Ann. Phys. (N.Y.) **272**, 130 (1999).
- [28] I. Affleck and J. B. Marston, Phys. Rev. B **37**, 3774 (1988); J. B. Marston and I. Affleck, Phys. Rev. B **39**, 11538 (1989).
- [29] P. A. Lee and N. Nagaosa, Phys. Rev. B **46**, 5621 (1992); P. A. Lee, N. Nagaosa, T.-K. Ng, and X.-G. Wen, Phys. Rev. B **57**, 6003 (1998).
- [30] W. Ratner and X.-G. Wen, Phys. Rev. Lett. **86**, 3871 (2001); X.-G. Wen, Phys. Rev. B **65**, 165113 (2002); W. Ratner and X.-G. Wen, Phys. Rev. B **66**, 144501 (2002).
- [31] P. W. Anderson, Science **235**, 1196 (1987).
- [32] T. Senthil and P. A. Lee, Phys. Rev. B **71**, 174515 (2005).
- [33] P. Ghaemi and T. Senthil, Phys. Rev. B **73**, 054415 (2006).
- [34] P. A. Lee, N. Nagaosa, and X.-G. Wen, Rev. Mod. Phys. **78**, 17 (2006); P. A. Lee, Rep. Prog. Phys. **71** 012501 (2008).
- [35] J. Alicea, Phys. Rev. B **78**, 035126 (2008).
- [36] M. Franz, Z. Tešanović, Phys. Rev. Lett. **87**, 257003 (2001); M. Franz, Z. Tešanović, O. Vafek, Phys. Rev. B **66**, 054535 (2002), I. Herbut, Phys. Rev. B **66**, 094504 (2002).
- [37] S. Hands, A. Kocić, and J. Kogut, Ann. Phys. **224**, 29, 1993.
- [38] C. J. Burden and A. N. Burkitt, Europhys. Lett. **3**, 545 (1987).
- [39] S. Kim, J. B. Kogut and M. P. Lombardo, Phys. Lett. **B502**, 345 (2001); S. Kim, J. B. Kogut and M. P. Lombardo, Phys. Rev. D **65**, 054015 (2002).

- [40] J. B. Kogut and C. G. Strouthos, Phys. Rev. D **67**, 034504 (2003); J. B. Kogut and C. G. Strouthos, Phys. Rev. D **71**, 094012 (2005).
- [41] B. Rosenstein, B. Warr, and H. Park, Phys. Rev. Lett. **62**, 1433 (1989).
- [42] T. A. DeGrand and D. Toussaint, Phys. Rev. D **22**, 2478 (1980).
- [43] J. L. Cardy, Nucl. Phys. **B170**, 369 (1980).
- [44] M. Göckeler, R. Horlsey, P. E. L. Rakow, and G. Schierholz, Phys. Rev. D **53**, 1508 (1996).
- [45] M. Salmhofer and E. Seiler, Commun. Math. Phys. **139**, 395 (1991); **146**, 637(E) (1992).
- [46] E. Dagotto, A. Kocić, and J. B. Kogut, Nucl. Phys. **B334**, 279 (1990).
- [47] S. Christofi and C. Strouthos, J. High Energy Phys. **0705**, 088 (2007).
- [48] K. Binder, Z. Phys. B **43**, 119 (1981).
- [49] M. Shifman and M. Ünsal, Phys. Rev. D **78**, 065004 (2008); E. Popitz and M. Ünsal, J. High Energy Phys. **12**, 011 (2009).
- [50] S. Hands, J. B. Kogut and B. Lucini, arXiv:hep-lat/0601001.
- [51] A. Concha, V. Staner and Z. Tešanović, Phys. Rev. B **79**, 214525 (2009); J. A. Bonnet, C. S. Fischer, and R. Williams, arXiv:1103.1578v1 [hep-ph].
- [52] S. Hands and I. O. Thomas, Phys. Rev. B **72**, 054526 (2005); S. Hands and I. O. Thomas, Phys. Rev. B **75**, 134516 (2007).
- [53] T. Senthil, V. Vishwanath, L. Balents, S. Sachdev, and M. A. P. Fisher, Science **303**, 1490 (2004); T. Senthil, L. Balents, S. Sachdev, A. Vishwanath, and M. A. P. Fisher, Phys. Rev. B **70**, 144407 (2004).